Supporting Information

Bifunctional $NiCo_2S_4$ Catalysts Supported on a Carbon Textile Interlayer for Ultra-stable Li-S Battery

Bo Liu,[a] Shaozhuan Huang,[a] Dezhi Kong,[a] Junping Hu, [a] Hui Ying Yang[a,] *

[a]*Pillar of Engineering Product Development, Singapore University of Technology and Design, 8 Somapah Road, Singapore, 487372*

*Corresponding author. Tel.: +65 6303 6663; Fax: +65 6779 5161. E-mail address: yanghuiying@sutd.edu.sg (H. Y. Yang).

Experimental Section

Theoretical calculation: all the calculations are based on DFT using the plane-wave pseudopotentials[1] with exchange-correlation of Perdew-Burke-Ernzerhof (PBE)[2, 3] formation as implemented in the Vienna Ab initio Simulation Package (VASP).[4] The effective onsite Coulomb interaction values used here are taken from the literatures: 6.4 eV for Ni[5] and 4.0 eV for Co[6] , with J =1 eV for both. A cutoff energy of 500 eV is employed for the plane wave expansion of the wave functions. The Brillouin zone is sampled with 3 × 5 × 1 Monkhorst-Pack k-point mesh[7] for the structural optimization. The convergence criteria for the total energy and ionic forces were set to 10^{-4} eV and 0.01 eV/Å, respectively. The construction with a 20 Å vacuum zone in the z direction to minimize the interactions between adjacent images.

Hydrothermal synthesis of $NiCo_2S_4$ nanosheets with large area and mesopores on CT: self-supported $NiCo_2S_4$ nanosheets with large area and mesopores on CT were prepared *via* a modified hydrothermal synthesis approach. In a typical process, a piece of CT with the customized size of 2.5 × 5.5 cm^2 was firstly activated with the concentrated HNO_3 solution for 24 h. Afterwards, the CT was thoroughly cleaned with DI and ethanol to remove the residual acids, followed by vacuum drying at 60 ℃ for 2 h. Meanwhile, a mixed solution of 60 mL DI water and 20 mL ethanol absolute of analysis degree was prepared consisting of 450 mg $Ni(NO_3)_2 \cdot 6H_2O$, 900 mg $Co(NO_3)_2 \cdot 6H_2O$, and 600 mg hexamethylenetetramine. The solution was thoroughly stirred until a transparent and light purple mixture was obtained. Then, the solution and the CT were transferred together into a Teflon-lined stainless-steel autoclave (100 mL) and maintained 100 ℃ for 8 h. After naturally cooling down, the sample was collected and washed with DI water and ethanol; meanwhile, the solution consisting of 80 ml DI water and 480 mg anhydrous Na_2S were prepared after thoroughly stirring. Afterwards, the sample and the solution were transferred together into a Teflon-lined stainless-steel autoclave again and keep the reaction temperature at 160 ℃ for 12 h. After naturally cooling down, the sample was washed with copious amount of DI water, followed by ethanol; then, it is dried in vacuum oven at 60 ℃ for 24 h to completely remove the residual moisture.

Preparation of MWCNT/S cathode with 75 % S loading: MWCNT from Sigma was directly used as received without further purification. In the typical melt-diffusion

method, the MWCNT and sulfur was mixed with the desired ratio in the mortar for 30 min, followed by heating in the ambient atmosphere at 155 ℃ for 12 h.

Materials Characterization: the morphology was studied through the Field-Emission Scanning Electron Microscope (FESEM, JSM-7600), equipped with the Energy Dispersive X-ray Spectroscopy (EDS, Oxford INCA EDS) analysis system. Crystalline phases were carried out with the X-Ray Diffraction (XRD, Bruker D8), equipped with Cu-Kα radiation. Lattice dynamics information was performed *via* the confocal Raman system with a 532 nm laser excitation source (WITec Instruments Corp, Germany). To further research morphologies and lattice structures, the Transmission Electron Microscope (TEM, 2100F) operated at an accelerating voltage of 200 kV was applied to the powder. The thermogravimetric analysis (TGA, DTG-60, Shimadzu) was conducted to tell the sulfur content in the cathode mix. In addition, the specific surface area of ultrasonicated $NiCo_2S_4$ was obtained by N_2 physisorption at 77 K using the Brunauer– Emmett–Teller (BET, TriStar II 3020, Micromeritics) method. The chemical composition and valence states of the samples were also studied by an X-ray photoelectron spectroscope (XPS, PHI Quantera II, Physical Electronics, Adivision of ULCAV-PHI).

Adsorption properties of Li_2S_6 for Li_2S_6/$NiCo_2S_4$ interaction study: Li_2S_6 was synthesized with Li_2S and sulfur in amounts corresponding to the nominal stoichiometry. Specifically, bulk S element and Li_2S in a molar ratio of 5:1 were added to a mixed solution of DOL/DME (1:1; v:v). The mixed solution was thoroughly stirred at 60 ℃ for 12 h under an argon atmosphere to obtain a $1/3$ M Li_2S_6 in DOL/DME stock solution. 40 mg of pure carbon textile and $NiCo_2S_4$@CT were added to each of diluted stock solution (8 μL in 2 mL of 1:1 DOL/DME). The mixtures were vigorously stirred to facilitate adsorption.

Cell assembly and electrochemical evaluation: symmetric electrochemical cells were assembled by the following procedure: the $NiCo_2S_4$@CT sheet was cut into a circle with diameter of ~1.8 cm. The thickness of the interlayer is around 0.33 mm, the density of the interlayer is around 150 g m^{-2} and the content of $NiCo_2S_4$ in the interlayer is around 7 wt%. The $NiCo_2S_4$ loading on one piece of interlayer is about 2.0 – 3.0 mg. CR2032-type coin cells were assembled in an Ar-filled glove box by using two $NiCo_2S_4$@CT sheets as the cathode and anode, a Celgard 2400 separator, and 50 μL

electrolyte of 1.0 M LiTFSI and 0.2 M Li_2S_6 in a 1:1 DOL/DME mixture. Lithium sulfur batteries were assembled with the different procedure: the cathode was homogenized in NMP with 80 wt% MWCNT/S, 10 wt% Super P, and 10 wt% polyvinylidene (PVDF), and slurry was evenly spread onto the Al foil to a loading of ~1.5 mg cm^{-2}; then, the coated electrodes were immediately put into the vacuum oven, followed by the heating process at 60 ℃ for 24 h. For comparison, thicker MWCNT/S electrodes with higher sulfur loading of 3.1 and 5.2 mg cm^{-2} were also prepared. Prior to the electrochemical measurements, all samples were assembled into a two-electrode configuration in an argon-filled glovebox with H_2O and O_2 concentration below 1.0 ppm. The electrolyte/sulfur ratio without interlayer is 10 $\mu L \cdot mg_S^{-1}$, and the electrolyte/sulfur ratio with interlayer is 20 $\mu L \cdot mg_S^{-1}$. The as-synthesized $NiCo_2S_4$@CT was directly sandwiched in the two-electrode cell configuration, where the interlayer was covered by the Celgard polypropylene separator to avoid short circuit in the CR2032 coin cell. 1.0 M LiTFSI was dissolved in the mixed solution of DOL/DME (1 : 1, v/v) with 0.2 M $LiNO_3$ as the stabilizer.

Electrochemical impedance spectroscopy (EIS) and cyclic voltammetry (CV) were performed on an electrochemical workstation (VMP3; Bio-logic, France), where the CV tests were carried out at sweep rate of 0.1 mVs^{-1}; while the impedance spectra were conducted in the frequency range between 100 kHz to 10 mHz with a perturbation amplitude of 5 mV. The galvanostatic charging/discharging was carried out on a battery tester (CHI-660C, Neware, China), where the rate performance was carried out in the voltage range of 1.7-2.8 V at current densities ranging from 0.1 to 3.0 C.

Figures

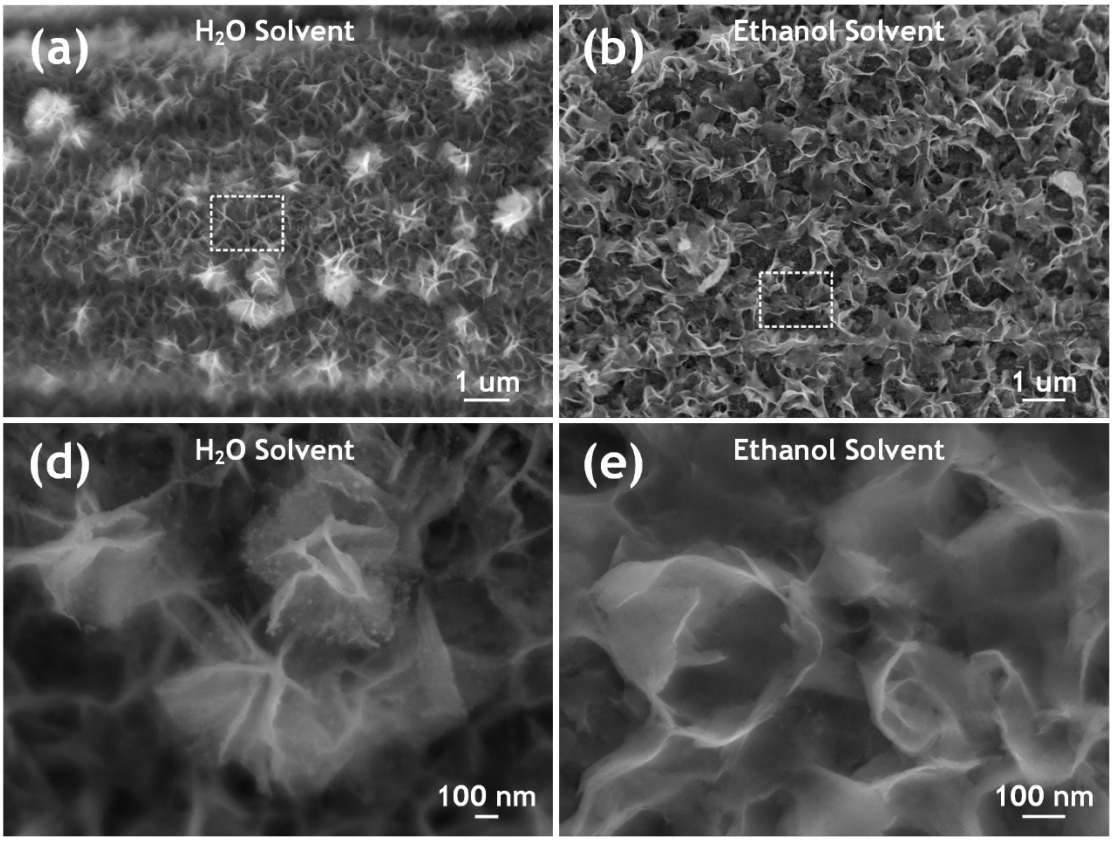

Figure S1. SEM images of carbon textile interlayer with $NiCo_2S_4$, dispersed by D.I. water/ethanol, separately.

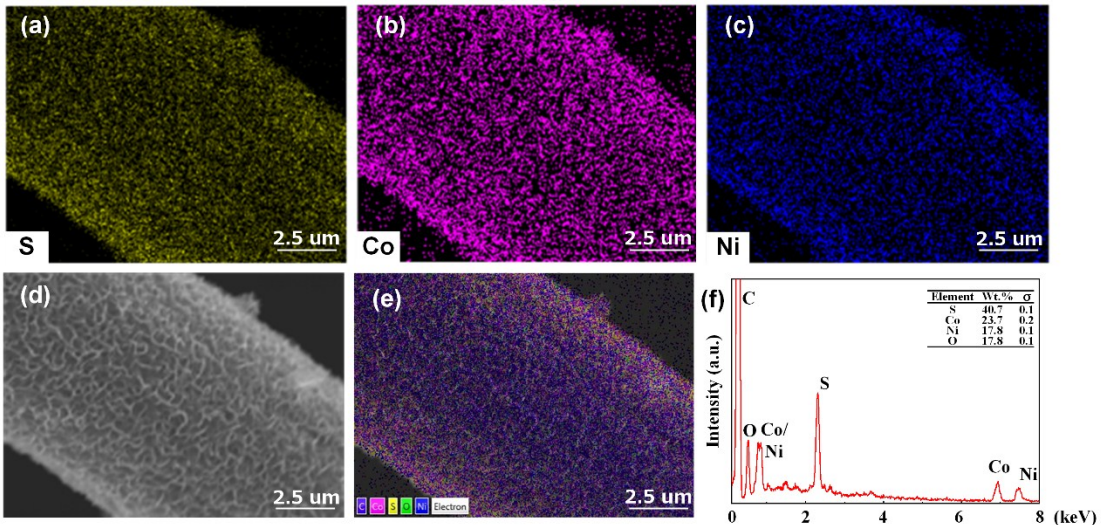

Figure S2. EDS Elemental mapping images of $NiCo_2S_4$@CT: (a) S, (b) Co, (c) Ni and the corresponding selected SEM image (d) and the mixed elemental mapping image (e). (f) The EDS elemental spectrum of $NiCo_2S_4$@CT.

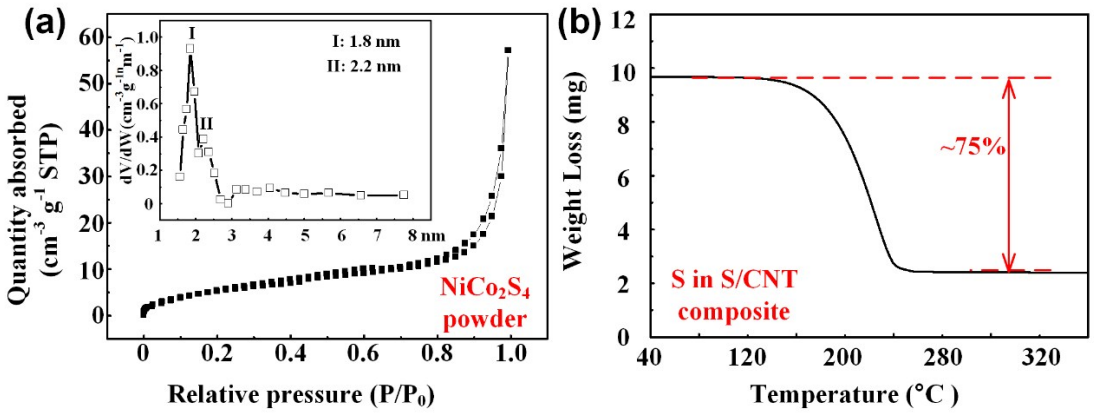

Figure S3. (a) TGA curve of the S content in the sulphur and carbon nanotube composite; (b) BET curves showing the nitrogen gas sorption isotherms at 77 K and pore size distribution of $NiCo_2S_4$ powders.

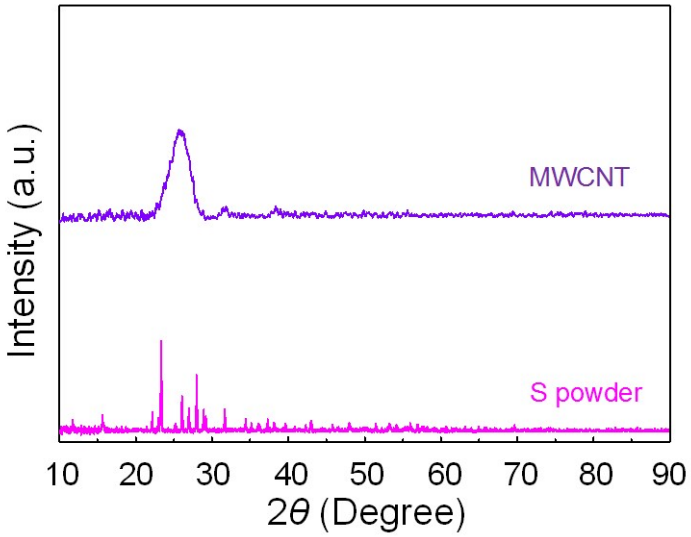

Figure S4. XRD patterns of MWCNT and sulphur powders.

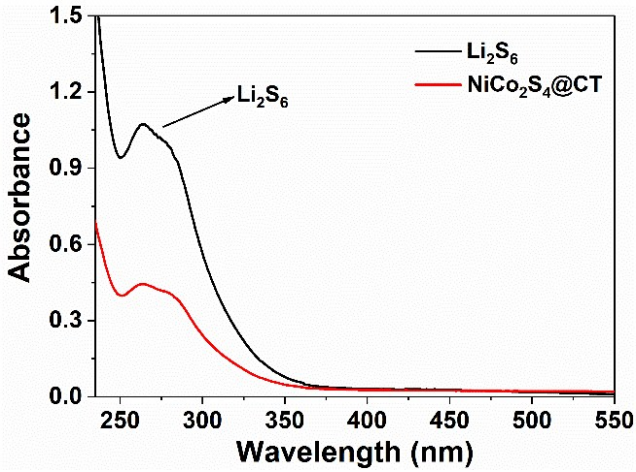

Figure S5. Ultraviolet-visible (UV) absorption spectra of Li_2S_6 solution before and after the addition of $NiCo_2S_4$@CT.

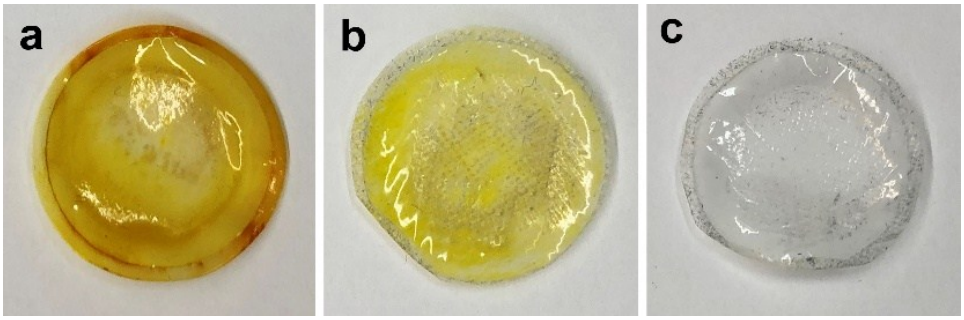

Figure S6. Photographs of the separators after cycling: (a) without interlayer, (b) bare CT, (c) $NiCo_2S_4$@CT.

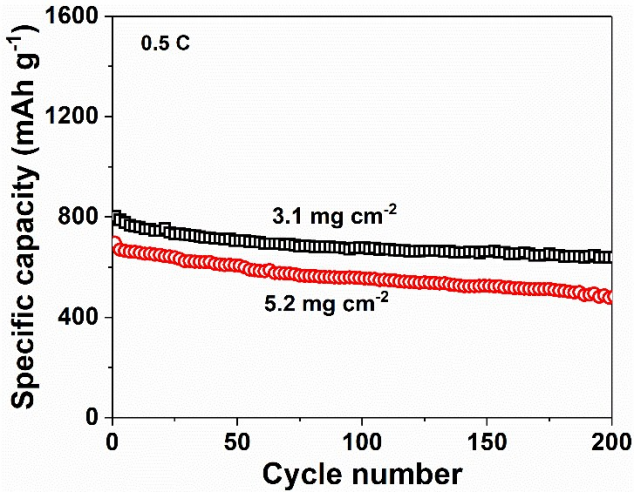

Figure S7. Cycling performance of battery with $NiCo_2S_4$ interlayer and different S loadings.

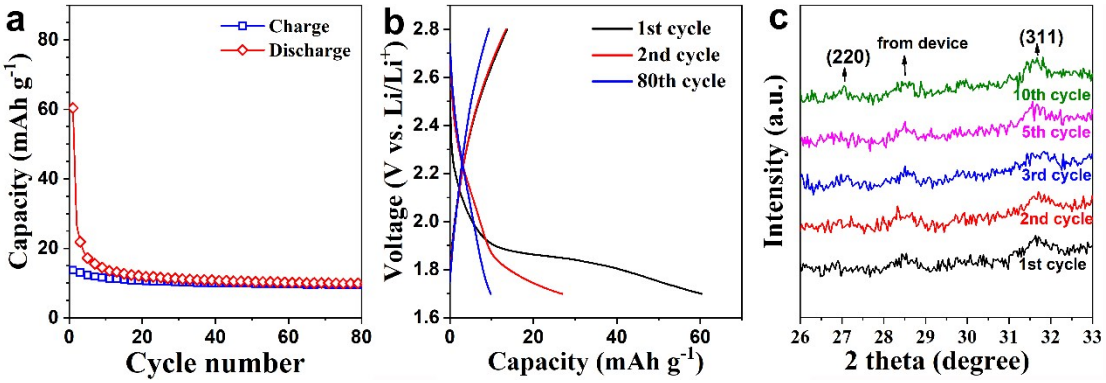

Figure S8. (a and b) Cycling performance of $NiCo_2S_4$ electrode at 100 mA g^{-1} in the voltage window of 1.7-2.8 V, (c) in situ XRD patterns at different cycles.

Table 1 Comparative table of decay rate during cycling between our work and the previous results

Sample	Decay rate/cycle	Cycle No.	Reference
S/CNT–$NiCo_2S_4$@CT interlayer	0.018% (0.5C)	500	Our work
WS_2/S–WS_2/CT interlayer	0.064% (0.5C)	500	[8]
S/CNT–ZnO/C interlayer	0.05% (2C)	200	[9]
CNFs@WS_2/S hybrids	0.0072% (0.2 C)	1500	[10]
C@Fe_3O_4/S hybrids	0.079% (0.5C)	200	[11]
S/Co_8S_9 nanoparticles	0.045% (0.2 C)	1500	[12]
S/CoS_2 nanoparticles	0.034% (2C)	2000	[13]

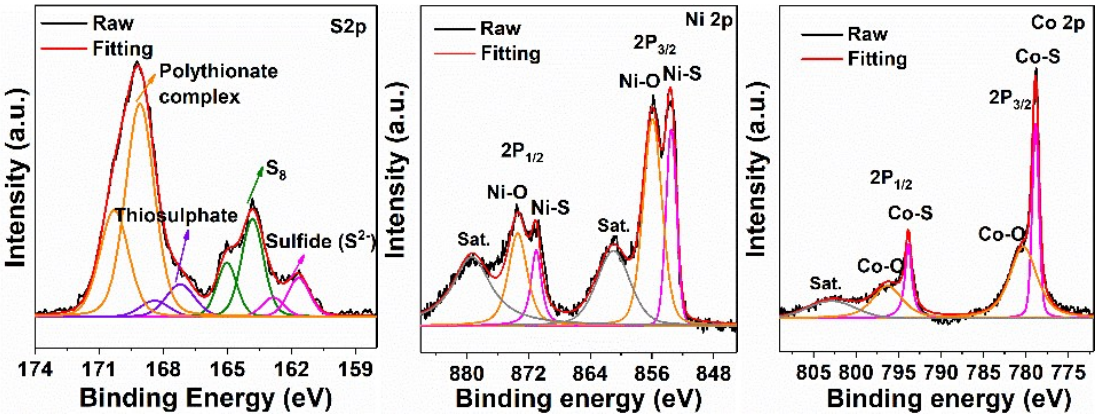

Figure S9. XPS spectra of the $NiCo_2S_4$ after 1500 cycles: (a) S 2p, (b) Ni 2p, (c) Co 2p.

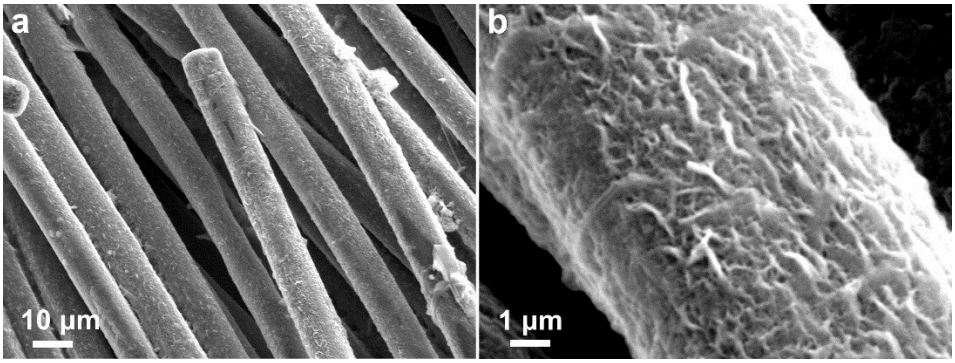

Figure S10. Ex situ SEM images of the $NiCo_2S_4$@CT interlayer after 100 cycles.

Reference:

[1] J. Ihm, A. Zunger, M. L. Cohen, *J. Phys. C: Solid state Phys.,* 1979, 12, 4409.

[2] J. P. Perdew, K. Burke, M. Ernzerhof, *Phys. Rev. Lett.,* 1996, 77, 3865.

[3] G. Kresse, D. Joubert, *Phys. Rev. B,* 1999, 59, 1758.

[4] G. Kresse, J. Furthmüller, *Phys. Rev. B,* 1996, 54, 11169.

[5] Wang, L.; Maxisch, T.; Ceder, G., *Physical Review B,* 2006, 73, 195107.

[6] Ritzmann, A. M.; Pavone, M.; Muñoz-García, A. B.; Keith, J. A.; Carter, E. A. *J. Mater. Chem. A,* 2014, 2, 8060- 8074.

[7] H.J. Monkhorst, J. D. Pack, *Phys. Rev. B,* 1976, 13, 5188.

[8]. Park, J., Yu, B. C., Park, J. S., Choi, J. W., Kim, C., Sung, Y. E., and Goodenough, J. B. *Adv. Energy Mater.,* 2017, 7, 11, 1602567.

[9]. Zhao, T., Ye, Y., Peng, X., Divitini, G., Kim, H.K., Lao, C.Y., Coxon, P.R., Xi, K., Liu, Y., Ducati, C. and Chen, R., *Adv. Fun. Mater.,* 2016, 26, 46, 8418-8426.

[10]. Lei, T., Chen, W., Huang, J., Yan, C., Sun, H., Wang, C., Zhang, W., Li, Y. and Xiong, J., *Adv. Energy Mater.,* 2017, 7, 4, 1601843.

[11]. He, J., Luo, L., Chen, Y. and Manthiram, A., *Adv. Mater.,* 2017. 29, 34, p.1702707.

[12]. Pang, Q., Kundu, D. and Nazar, L.F. *Materials Horizons,* 2016. 3, 2, 130-136.

[13]. Yuan, Z., Peng, H.J., Hou, T.Z., Huang, J.Q., Chen, C.M., Wang, D.W., Cheng, X.B., Wei, F. and Zhang, Q., *Nano letters,* 2016. 16, 1, 519-527.